Phase Diagram of the Two-Dimensional Homogeneous Electron Gas

Neil D. Drummond and Richard J. Needs

TCM Group, Cavendish Laboratory, University of Cambridge

ESDG Meeting

Wednesday 13th February, 2008

Two-Dimensional Homogeneous Electron Gas (I)

- 2D HEG: set of electrons moving in 2D in a uniform, inert, neutralising background.

- Hamiltonian (for finite system):

$$\hat{H} = \sum_i -\frac{1}{2}\nabla_i^2 + \sum_{j>i} v_E(\mathbf{r}_{ij}) + \frac{N v_M}{2}.$$

  Infinite-system GS energy per particle depends only on the **density** (specified by radius r_s of circle containing one electron on average) and **spin polarisation** [$\zeta = (N_\uparrow - N_\downarrow)/N$].

- Physical realisations:

  - *Electrons on metal surfaces.* E.g. Cu [111].
  - *Electrons on droplets of liquid He.* Held in place by image charges
  - *Inversion layers in MOS devices.* Can easily tune density. Electrons far from dopants; fewer complications due to disorder; technologically important.

Two-Dimensional Homogeneous Electron Gas (II)

- HEG is simplest fully interacting quantum many-body system.
- QMC is the only accurate method available for studying its ground-state properties.
- We have carried out QMC studies of the 2D HEG:
  1. We have calculated the zero-temperature phase diagram.[1]
  2. We have calculated the PCF, structure factor and momentum distribution.[2]
- Our data will be of interest to
  - Experimentalists looking for ferromagnetism and Wigner crystallisation in low-density 2D HEGs.
  - Theorists interested in constructing 2D XC functionals for DFT calculations.
- Our calculations are more accurate than previous ones because of (i) a better treatment of finite-size errors; (ii) a more accurate nodal surface; (iii) Darwin.

[1] N. D. Drummond and R. J. Needs, submitted to Phys. Rev. Lett. (2008).

[2] N. D. Drummond and R. J. Needs, to be submitted to Phys. Rev. B (2008).

Wigner Crystallisation in 2D (I)

- Kinetic energy dominates at high density: *form Fermi fluid to minimise it.*
- Potential energy dominates at low density: *form Wigner crystal to minimise it.*
- Wigner crystals have been observed on the surface of liquid helium[3] and in inversion layers in MOSFET devices[4].
- 2D Wigner crystals could be of use in quantum computing devices.[5]
- Previous QMC studies[6] indicate that fluid–crystal transition occurs somewhere between $r_s = 25$ and 40 a.u.
- Can we be more precise?

---

[3] C. C. Grimes and G. Adams, Phys. Rev. Lett. **42**, 795 (1979).

[4] E. Y. Andrei *et al.*, Phys. Rev. Lett. **60**, 2765 (1988); R. L. Willett *et al.*, Phys. Rev. B **38**, 7881 (1988).

[5] P. M. Platzman & M. I. Dykman, Science **284**, 1967 (1999); P. Glasson *et al.*, Phys. Rev. Lett. **87**, 176802 (2001).

[6] B. Tanatar & D. M. Ceperley, Phys. Rev. B **39**, 5005 (1989); F. Rapisarda & G. Senatore, Aust. J. Phys. **49**, 161 (1996).

Hartree–Fock Theory of 2D Wigner Crystals (I)

- Full Hartree-Fock calculations using a PW basis have been performed.[7] Here we derive an approximate analytic theory.

- At low densities Wigner crystal orbitals are of form

$$\phi_{\mathbf{R}}(\mathbf{r}) = \exp(-C|\mathbf{r} - \mathbf{R}|^2)$$

  where $\mathbf{R}$ is a lattice site and C is an optimisable parameter.

- (This is like the Einstein approximation to the ZPE of a crystal.)

- Exchange effects are negligible in low-density limit. Approximate Slater determinant by a Hartree product.

[7] J. R. Trail *et al.*, Phys. Rev. B **68**, 045107 (2003).

Hartree–Fock Theory of 2D Wigner Crystals (II)

- Total energy per electron is sum of kinetic energy and Hartree energy (electrostatic energy of a periodic array of Gaussian charge distributions) minus the self energy of each Gaussian charge distribution:

$$E = C - \frac{\sqrt{\pi C}}{2} + \frac{1}{r_s^2} \sum_{\mathbf{G}\neq\mathbf{0}} \frac{1}{G} \exp\left(\frac{-G^2}{4C}\right).$$

- Demand that energy is minimised with respect to C:

$$\begin{aligned} 0 = \left(\frac{\partial E}{\partial C}\right)_{r_s} &= 1 - \frac{1}{4}\sqrt{\frac{\pi}{C}} + \frac{\pi}{4AC^2} \sum_{\mathbf{G}\neq\mathbf{0}} G \exp\left(-\frac{G^2}{4C}\right). \\ &\simeq 1 - \frac{1}{4}\sqrt{\frac{\pi}{C}} + \frac{1}{8C^2} \int_{\left(\frac{4\pi}{A}\right)^{1/2}}^{\infty} G^2 \exp\left(-\frac{G^2}{4C}\right) \, dG \\ &\simeq 1 - \frac{1}{3C^2 r_s^3} + \mathcal{O}(r_s^{-1/4}), \end{aligned}$$

Hartree–Fock Theory of 2D Wigner Crystals (III)

- Hence the optimal C is $C = r_s^{-3/2}/\sqrt{3}$.

- Integrate $(\partial E/\partial C)_{r_s}$ w.r.t. C. At low densities E must tend to Madelung energy M/r_s, so integration constant is M/r_s. Insert optimal value of C:

$$E \approx \frac{2}{\sqrt{3} r_s^{3/2}} + \frac{M}{r_s}.$$

r_s (a.u.)	Kinetic energy (10^{-4} a.u.)		
	Analytic Approx.	Simple model	Full UHF
10	182.5741858	169.5220370	165.9043241
20	64.54972244	56.79743741	56.19776102
30	35.13641845	30.03820383	29.87538105
40	22.82177323	19.18376842	19.11263264
50	16.32993162	13.57764993	13.53238132
75	8.888888889	7.275719420	7.245278062
100	5.773502692	4.685191601	4.633373199

Hartree–Fock Theory of 2D Wigner Crystals (IV)

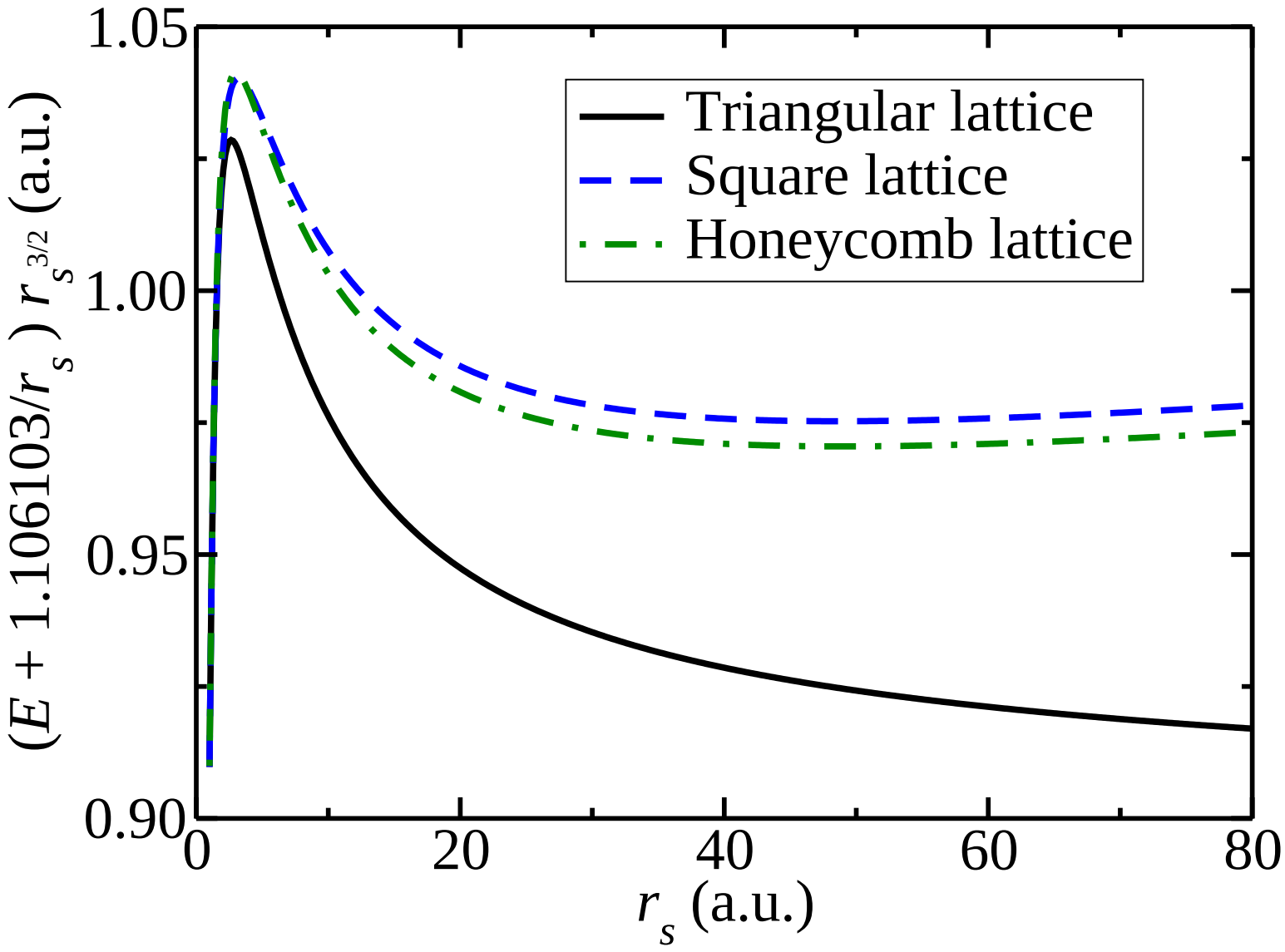

Triangular lattice has lowest energy in HF theory.

Magnetic Behaviour of the Fermi Fluid

- Bloch transition: para. fluid favoured at high density (want to minimise KE); ferro. fluid favoured at low density (keep electrons apart to minimise XC energy).
- Hartree–Fock theory: Bloch transition at $r_s = 2.01$ a.u. No region of stability for ferromagnetic fluid.
- VMC[8]: Bloch transition at $r_s = 13(2)$ a.u.; crystallisation at $r_s = 33(2)$ a.u.
- DMC[9]: Bloch and crystallisation transitions at $r_s = 37(5)$ a.u.
- DMC[10]: Bloch transition at $r_s = 20(2)$ a.u. and crystallisation at $r_s = 34(4)$ a.u.
- Experiment[11]: "Possible evidence" of ferromagnetism at $r_s = 7.6$ a.u.

---

[8] D. Ceperley, Phys. Rev. B **18**, 3126 (1978).
[9] B. Tanatar and D. M. Ceperley, Phys. Rev. B **39**, 5005 (1989).
[10] F. Rapisarda and G. Senatore, Aust. J. Phys. **49**, 161 (1996).
[11] A. Ghosh, C. J. B. Ford, M. Pepper, H. E. Beere and D. A. Ritchie, Phys. Rev. Lett. **92**, 116601 (2004).

Fermi Fluid: PBC, TBC and TABC

- Orbitals for Fermi fluid:
$$\phi_{\mathbf{k}}(\mathbf{r}) = \exp(i\mathbf{k}\cdot\mathbf{r}).$$

- Periodic boundary conditions: $\{\mathbf{k}\}$ are simulation-cell $\mathbf{G}$-vectors.

- *Single-particle finite-size effects:* Increase N at fixed density; grid of $\mathbf{G}$-vectors gets finer; energy per electron jumps as shells of $\mathbf{G}$ vectors pass through Fermi line.

- Twisted boundary conditions: $\mathbf{k}$ are simulation-cell $\mathbf{G}$ vectors offset by $\mathbf{k}_s \in$ 1st BZ of simulation cell.

- Twist averaging: average over all $\mathbf{k}_s$. Replaces grid of $\mathbf{k}$ by a Fermi area (equal to area of Fermi circle), greatly reducing single-particle finite-size effects. Shape of Fermi line isn't quite right: gives negligibly small positive bias to KE.

- Previous QMC studies of 2D HEG have not used twist averaging.

Static Structure Factors

Static structure factor:

$$S(\mathbf{r}, \mathbf{r}') = \frac{A}{N} \langle [\hat{\rho}(\mathbf{r}) - \rho(\mathbf{r})][\hat{\rho}(\mathbf{r}') - \rho(\mathbf{r}')] \rangle$$

where $\hat{\rho}(\mathbf{r}) = \sum_i \delta(\mathbf{r} - \mathbf{r}_i)$ is the density operator, $\rho(\mathbf{r}) = \langle \hat{\rho}(\mathbf{r}) \rangle$ is the density and A is the area of the simulation cell.

Translationally averaged structure factor:

$$S(\mathbf{r}) = \frac{1}{A} \int_A S(\mathbf{r}' + \mathbf{r}, \mathbf{r}') \, d\mathbf{r}'.$$

Fourier transform of the translationally averaged structure factor:

$$S(\mathbf{G}) = \frac{1}{N} \left(\langle \hat{\rho}(\mathbf{G}) \hat{\rho}^*(\mathbf{G}) \rangle - \rho(\mathbf{G}) \rho^*(\mathbf{G}) \right),$$

where $\hat{\rho}(\mathbf{G}) = \sum_i \exp(-i\mathbf{G} \cdot \mathbf{r}_i)$ is the Fourier transform of the density operator.

Hartree and XC Energies

$$\begin{aligned}
\left\langle \hat{V}_{\mathrm{Ew}} \right\rangle &= \frac{N v_M}{2} + \frac{\int |\Psi(\mathbf{R})|^2 \frac{1}{2} \sum_{i \neq j} v_E(\mathbf{r}_i - \mathbf{r}_j)\, d\mathbf{R}}{\int |\Psi|^2\, d\mathbf{R}} \\
&= \frac{1}{2} \int \int \left[\rho(\mathbf{r}, \mathbf{r}') - \rho(\mathbf{r})\rho(\mathbf{r}')\right] \left[v_E(\mathbf{r} - \mathbf{r}') - v_M\right]\, d\mathbf{r}\, d\mathbf{r}' \\
&\quad + \frac{1}{2} \int \int v_E(\mathbf{r} - \mathbf{r}')\rho(\mathbf{r})\rho(\mathbf{r}')\, d\mathbf{r}\, d\mathbf{r}' \\
&= \frac{N}{2} \left(\sum_{\mathbf{G} \neq \mathbf{0}} \frac{2\pi}{A|\mathbf{G}|} \left[S(\mathbf{G}) - 1\right] + v_M \right) + \sum_{\mathbf{G} \neq \mathbf{0}} \frac{\pi A}{|\mathbf{G}|} \rho(\mathbf{G})\rho^*(\mathbf{G}),
\end{aligned}$$

where $\rho(\mathbf{r}, \mathbf{r}') = \left\langle \sum_{i \neq j} \delta(\mathbf{r} - \mathbf{r}_i)\delta(\mathbf{r}' - \mathbf{r}_j) \right\rangle$ is the pair density.

First term: exchange-correlation energy (interaction of electrons with their XC holes).

Second term: Hartree energy (interaction of charge densities). **Zero for HEG**.

Finite-Size Effects in 2D (I)

Old assumption: finite-size errors are due to slow convergence of $v_E(\mathbf{r})$ to $1/r$ in XC energy. (This is main cause of finite-size effects at typical densities in 3D.)

Can cure this "problem" by using *model periodic Coulomb* interaction. But it was found that MPC doesn't change energies much in 2D.[12]

Alternative approach for curing the "problem": finite-size error is due to summation rather than integration over $\mathbf{G}$ in reciprocal-space expression for interaction energy.[13]

Poisson summation formula: $[1/(2\pi)^3] \int f(\mathbf{k})\, d\mathbf{k} = (1/A) \sum_{\mathbf{G}} f(\mathbf{G}) - \sum_{\mathbf{R}\neq\mathbf{0}} f(\mathbf{R})$.

So, if XC hole [and hence $S(k)$] has converged, finite-size correction is zero in 2D because $\lim_{\mathbf{k}\to\mathbf{0}} v_E(k)S(k) = 0$ (unlike 3D).[14]

New understanding[14]: 2D finite-size errors are caused by (i) slow convergence of the XC hole (screening is reduced in 2D) and (ii) neglect of long-ranged correlations in the KE.

---

[12] B. Wood, W. M. C. Foulkes, M. D. Towler and N. D. Drummond, J. Phys.: Condens. Matter **16**, 891 (2004).

[13] S. Chiesa, D. M. Ceperley, R. M. Martin and M. Holzmann, Phys. Rev. Lett. **97**, 076404 (2006).

[14] N. D. Drummond, R. J. Needs, A. Sorouri and W. M. C. Foulkes, to be submitted to Phys. Rev. B (2008).

Finite-Size Effects in 2D (II)

- Long-ranged nonoscillatory behaviour of the XC hole is known analytically[15]: $\rho_{\mathrm{xc}}(r) = -\tilde{\Lambda} r^{-7/2}$.
- Hence the XC charge outside radius r is $\tilde{Q} = -4\pi\tilde{\Lambda}/(3r^{3/2})$.
- Infinite-system XC charge outside finite simulation cell is ignored.
- So the error in the total Ewald energy due to the missing tail of the XC hole is

$$\Delta V_{\mathrm{Ew}} \approx -\frac{N}{2}\int_{R_A}^{\infty} \frac{1}{A}\frac{4\pi\tilde{\Lambda}}{3r^{5/2}} 2\pi r\, dr = \mathcal{O}(N^{-1/4}),$$

  where R_A is the radius of a circle of area A.
- Error resulting from distortion of XC hole inside the simulation cell is of the same order (can estimate by adding "missing" charge $\tilde{Q}$ in sensible fashion).

[15] P. Gori-Giorgi *et al.*, Phys. Rev. B **70**, 115102 (2004).

Finite-Size Effects in 2D (III)

- RPA: exact long-ranged correlation described by $\exp[\sum_{i>j} u(r_{ij})]$ in Jastrow factor.
- Write "TI" estimator of KE $\langle(-1/4)\nabla^2 \log(\Psi)\rangle$ in reciprocal space.
- Finite-size error in the TI estimate can be regarded as a difference between a sum and an integral, *à la* the Ewald energy.[16]
- Leading-order KE correction is due to omission of $\mathbf{G} = \mathbf{0}$ term in sum.
- Use analytic RPA expression for $u(k)$ at small k and integrate over area of $(2\pi)/A$ to obtain missing contribution to KE.
- Error in total KE goes as $\mathcal{O}(N^{-1/4})$.[17]

[16] S. Chiesa, D. M. Ceperley, R. M. Martin and M. Holzmann, Phys. Rev. Lett. **97**, 076404 (2006).

[17] N. D. Drummond, R. J. Needs, A. Sorouri and W. M. C. Foulkes, to be submitted to Phys. Rev. B (2008).

Finite-Size Effects in 2D (IV)

- Both sources of finite-size error in the 2D energy per electron go as $\mathcal{O}(N^{-5/4})$. So we should extrapolate energies to infinite system size using

$$E_N = E_\infty - bN^{-5/4}.$$

- Previous QMC studies have incorrectly used $N^{-3/2}$ for crystals and N^{-1} for fluid.

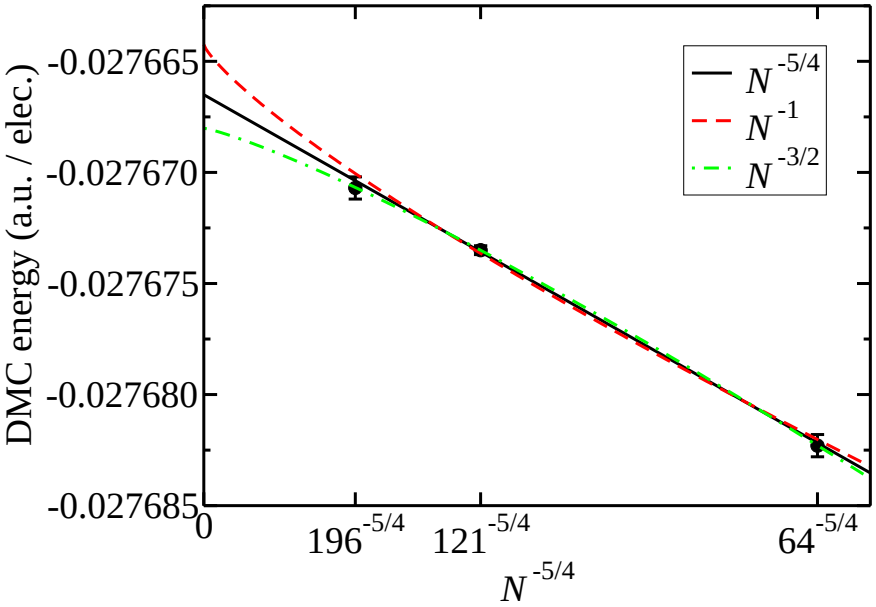

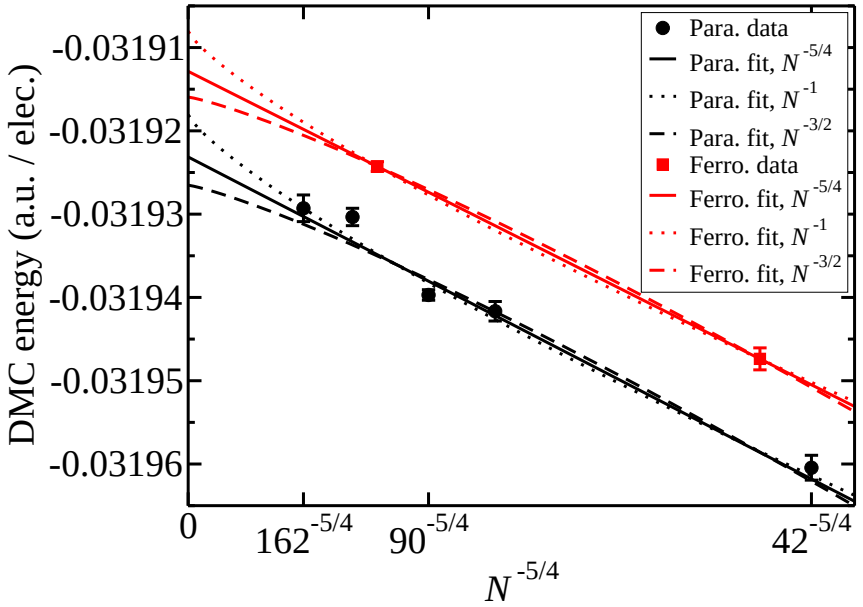

Left: crystal extrapolation at $r_s = 35$ a.u.; right: fluid extrapolation at $r_s = 30$ a.u.

Backflow Transformation

- Evaluate Slater wave function at quasiparticle coordinates related to actual electron coordinates by electron–electron backflow functions.[18]

- Moves nodal surface of wave function; can therefore improve the fixed-node DMC energy.

- At $r_s = 30$ a.u., BF lowers fluid DMC energy by 36(3) μHa per electron and lowers crystal DMC energy by 1.0(4) μHa per electron. (DMC energies extrapolated to zero time step and infinite system size.)

- Backflow is significant for the fluid, but not for the crystal, where electrons are already kept apart by localisation on lattice sites.

- Antiparallel-spin BF functions are much longer ranged than parallel-spin functions. Parallel spins are already kept away from each other by wave function antisymmetry.

[18] P. López Ríos, A. Ma, N. D. Drummond, M. D. Towler and R. J. Needs, Phys. Rev. E **74**, 066701 (2006).

Optimisation of Crystal Orbitals

Only parameter affecting crystal nodal surface: Gaussian exponent C. Minimise DMC energy w.r.t. C to minimise fixed-node error.

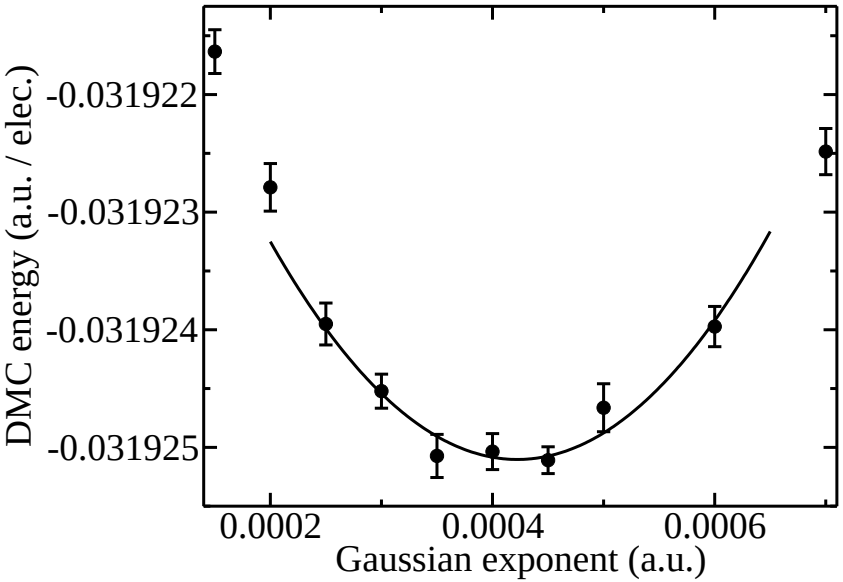

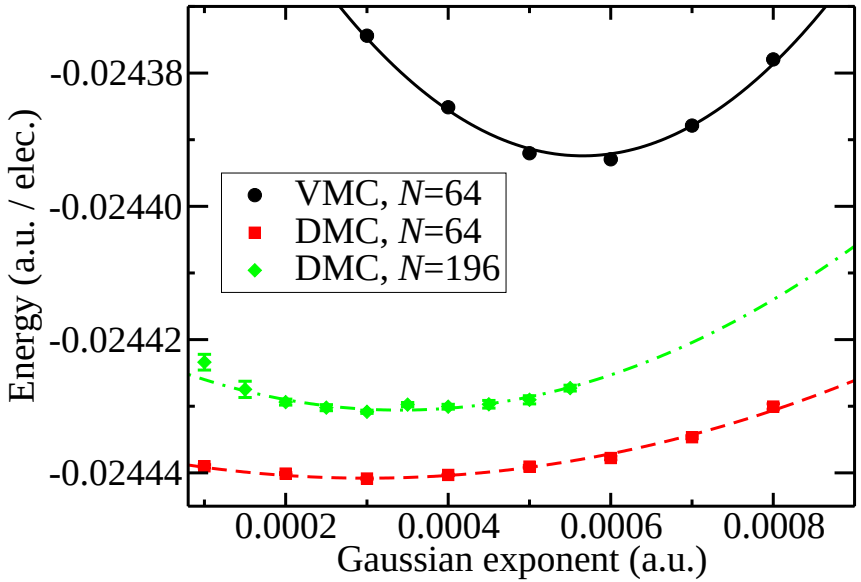

DMC energy against C at $r_s = 30$ a.u. (left) and $r_s = 40$ a.u. (right).

Optimal exponent is $C_{\mathrm{DMC}} = 0.071 r_s^{-3/2}$.
CF, VMC exponent is $C_{\mathrm{VMC}} = 0.15 r_s^{-3/2}$ and HF exponent is $C_{\mathrm{HF}} = 0.46 r_s^{-3/2}$.

Time-Step and Population-Control Biases

Population-control bias is bad at low density.[19]

Use about 1600 configurations to make population-control bias negligible.

Time-step bias is linear; extrapolate DMC energies to zero time step.

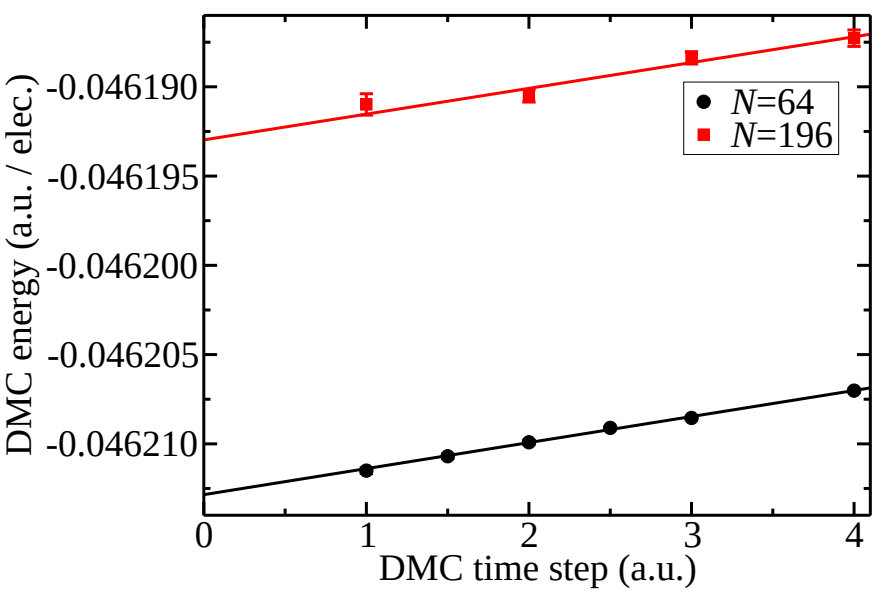

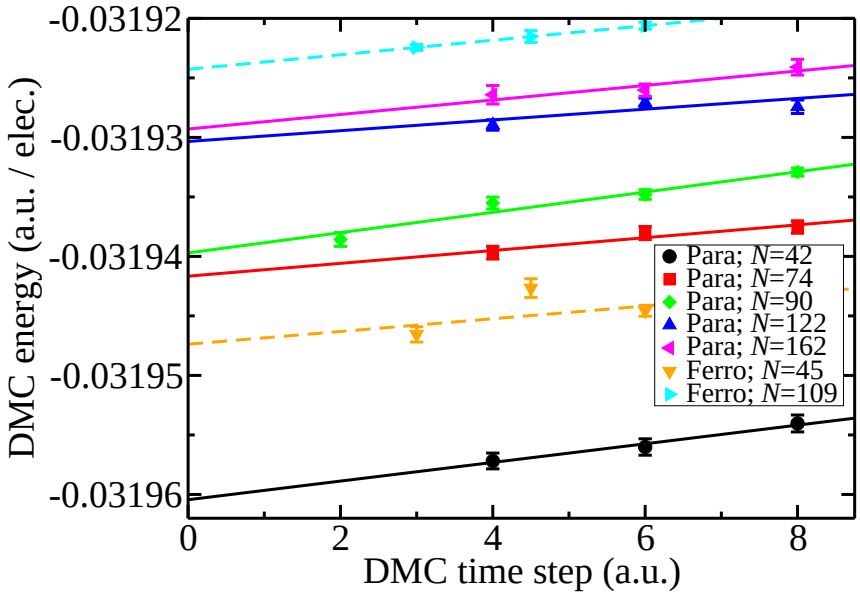

DMC energy against time step for a crystal at $r_s = 20$ a.u. (left) and fluid at $r_s = 30$ a.u. (right).

[19] N. D. Drummond, Z. Radnai, J. R. Trail, M. D. Towler and R. J. Needs, Phys. Rev. B **69**, 085116 (2004).

2D HEG Energy Diagram (I)

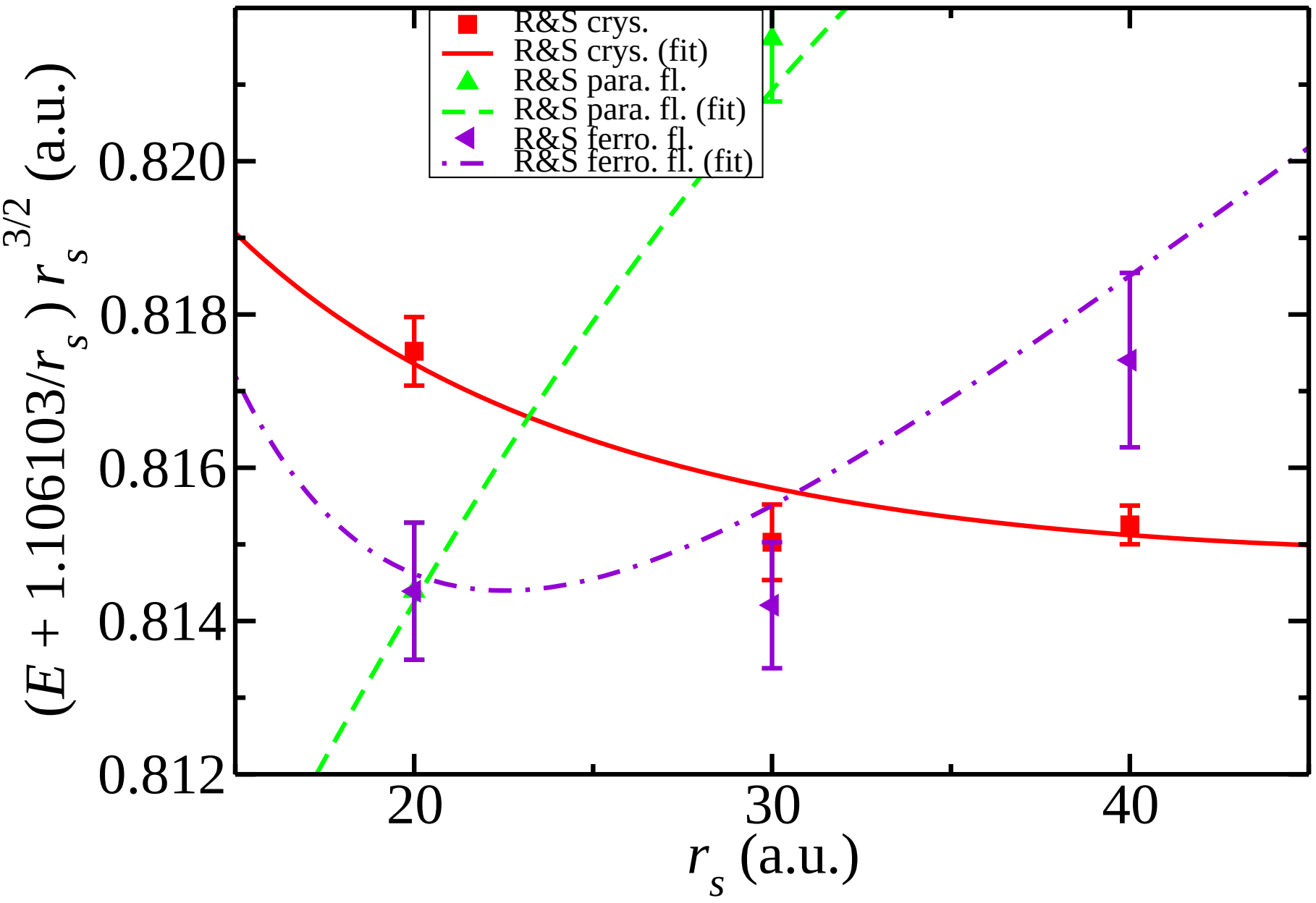

2D HEG Energy Diagram (I)

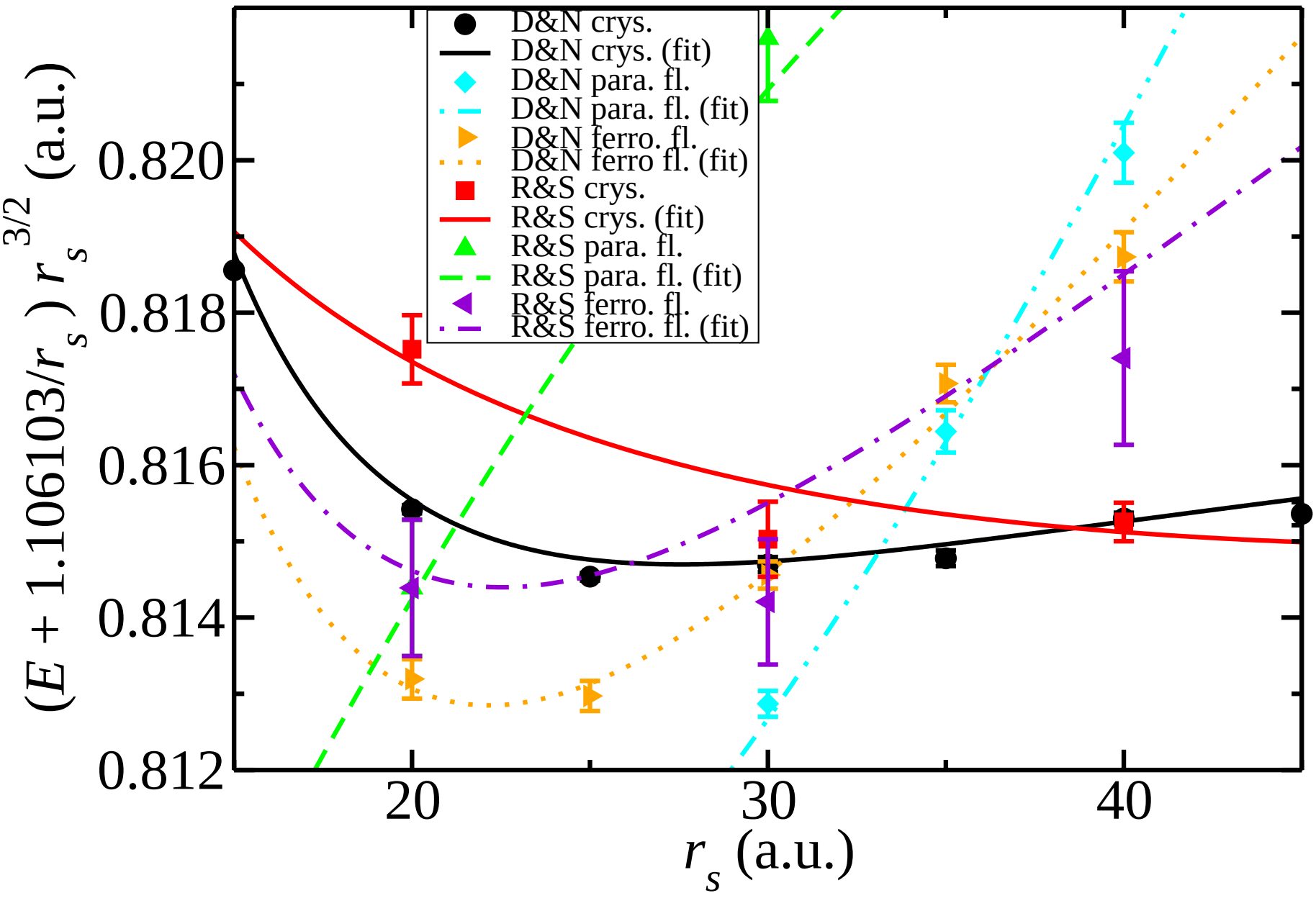

2D HEG Energy Diagram (II)

- Fully polarised fluid is never stable.
- Wigner crystallisation occurs at $r_s = 33 \pm 1$ a.u.
- At $r_s = 35$ a.u., the energy of a fluid with $\zeta = 2/5$ agrees with the paramagnetic and ferromagnetic fluid energies. Very unlikely that a region of stability for a partially polarised fluid exists.
- Phase transitions in 2D HEG cannot be first order.[20]
- It's energetically favourable to form boundaries between macroscopically separated phases, so a "microemulsion" is formed at crystallisation density.
- Doesn't affect basic features of phase diagram; just blurs boundaries.

[20] B. Spivak and S. A. Kivelson, Phys. Rev. B **70**, 155114 (2004); R. Jamei *et al.*, Phys. Rev. Lett. **94**, 056805 (2005).

Hybrid Phases

- It's been alleged that there exist hybrid phases that are neither fluid nor crystal[21].
- Orbitals are long-ranged Wannier functions.
- Have tried using orbitals of the form

$$\phi_{\mathbf{R}}(\mathbf{r}) = \exp\left(-C|\mathbf{r}-\mathbf{R}|^2\right) + \sum_S c_S \sum_{\mathbf{G}\in S} \cos[\mathbf{G}.(\mathbf{r}-\mathbf{R})],$$

  where C and the c_S are optimisable. S runs over stars of $\mathbf{G}$ vectors. This form of orbital can describe the proposed hybrid phase (and the crystal phase).

- Have looked, but haven't found the hybrid phase. Does it exist?
- Fact that fluid–crystal transition is from a paramagnetic fluid rather than a ferromagnetic one makes hybrid phase more unlikely.

[21] H. Falakshahi and X. Waintal, Phys. Rev. Lett. **94**, 046801 (2005); X. Waintal, Phys. Rev. B **73**, 075417 (2006).

Conclusions

- *There is no region of stability for a ferromagnetic Fermi fluid in 2D.*
- *Wigner crystallisation occurs at $r_s = 33 \pm 1$ a.u. in 2D.*
- *Have looked for a recently proposed "hybrid" phase. Didn't find it.*
- *Have calculated structure factors, pair-correlation functions and momentum distributions.* Didn't talk about them today, but I'll tell you *all* about them next time someone pulls out of their ESDG slot at short notice. . . **So don't do this.**

Acknowledgements

Financial support was received from Jesus College, Cambridge and the Engineering and Physical Sciences Research Council.

Computing resources were provided by the Cambridge High Performance Computing Service.